coatings

MDPI

Communication

The Influence of Site of Co and Holes in PCD Substrate on Adhesive Strength of Diamond Coating with PCD Substrate

Cen Hao and Guoliang Liu *

School of Information Technology, Jiangsu Open University, Nanjing 210036, China; haocen@jsou.edu.cn
* Correspondence: liuguol@jsou.edu.cn

Abstract: Polycrystalline diamond (PCD) prepared by the high temperature and pressure method often uses Co as a binder, which had a detrimental effect on the cutting performance of PCD, thus Co needed to be removed. However, the removal of Co would cause residual holes and also make the cutting performance of PCD poorer. To address this issue, hot filament chemical vapor deposition (HFCVD) was used. During deposition, the residual holes cannot be filled fully, and Co would diffuse to the interface between CVD diamond coatings and the PCD substrate, which influenced the adhesive strength of the diamond coating with the PCD substrate. In order to investigate the influencing mechanism, both experiments and the density functional theory (DFT) calculations have been employed. The experimental results demonstrate that Co and the holes in the interface would reduce the interfacial binding strength. Further, we built interfacial structures consisting of diamond (100), (110), (111) surfaces and PCD to calculate the corresponding interfacial binding energy, charge density and charge density difference. After contrast, for Co and the holes located on the (110) surface, the corresponding interfacial binding energy was bigger than the others. This means that the corresponding C-C covalent bond was stronger, and the interfacial binding strength was higher. Based on this, conducting cobalt removal pretreatment, optimizing the PCD synthetic process and designing the site of Co can improve the performance of the PCD substrate CVD diamond coating tools.

Keywords: DFT calculations; polycrystalline diamond; diamond coating; adhesive strength

Citation: Hao, C.; Liu, G. The Influence of Site of Co and Holes in PCD Substrate on Adhesive Strength of Diamond Coating with PCD Substrate. *Coatings* **2024**, *14*, 1. https://doi.org/10.3390/coatings14010001

Academic Editor: Fabien Bénédic

Received: 29 November 2023
Revised: 12 December 2023
Accepted: 14 December 2023
Published: 19 December 2023

1. Introduction

Polycrystalline diamond (PCD) is a kind of superhard material with excellent performance. It is formed by sintering micron-sized diamond particles and binder under high temperature and high-pressure conditions. Thus, the PCD can be widely used in the processing field of non-ferrous metals alloys, ceramics, difficult-to-machine composite materials, etc. [1–4]. In the sintering process of PCD under high pressure, Co is often used as the metal binder [5–8]. Co makes diamond easy to transform to graphite, which greatly reduces the adhesive strength between PCD and films [9–13]. Therefore, in order to improve the performance and service life of the tool, it is imperative to remove Co from PCD [14–17]. After the removal of Co, the original position of Co will produce holes. To address the issue of PCD's poor cutting performance, the holes remaining on the PCD surface after cobalt removal were filled using hot filament chemical vapor deposition (HFCVD). During deposition, some of the holes were full of diamond, but some holes deep in PDC still exist [18]. Besides, the Co element would diffuse to the interface between the PCD and CVD diamond coatings. Both would affect the adhesive strength of diamond coatings.

There are many factors that affected the adhesive strength of CVD diamond coatings, from the materials of substrate, pre-treatment of substrate [19–21], to deposition parameters [22,23] and post deposition treatment [24], all of which could improve the adhesive strength of CVD diamond coatings. Xiaogang Jian [25–29] used first principles based upon density functional theory (DFT) to investigate the influence of cobalt binding phase, crystal

orientation and line defect in cemented carbide substrate on the adhesive strength of the diamond coating. He found that the Co element can transfer the charges near the interface of WC/diamond model when the magnetic Co element exists at the WC/diamond interface. As a result, the cobalt binding phase in cemented carbide substrate can weaken the adhesive strength of diamond coating. And the adhesive strength of the model of (100) crystal orientation is maximal. Besides, the surface energy of cemented carbide substrate increases at first and then decreases as the line defect ratio in the substrate surface grows. Based on the conclusions above, it was necessary to study the influence of Co in PCD substrate and holes on adhesive strength of diamond coating with PCD substrate.

In this article, we firstly performed the indentation experiments and found that the Co and holes would reduce the adhesive strength of diamond coatings. Then, in order to explain the influence mechanism from an electronic perspective, the first-principles projector augmented wave (PAW) pseudopotential method within the generalized gradient approximation (GGA) based on the density functional theory (DFT) was employed. We used Device Studio software (2023A) to build different PCD/diamond and PCD-holes/diamond interfacial structures based on different crystal surfaces ((100), (110), (111)). The DS-PAW software (2023A) package was used to obtain the most stable interfacial structure [30]. Further, the corresponding interfacial binding strength, charge density and charge density difference were calculated. The calculation results in this article demonstrated that during the synthesis of PCD, we could regulate the site of the Co binding phase in PCD, or to remove the Co elements on a certain crystal surface during the pretreatment process, or to fill the holes in some sites when depositing, thus the interface binding strength between the PCD substrate and the diamond coatings could be improved. In addition, it could also reveal the theoretical mechanism of the adhesive strength of CVD diamond coatings.

2. Experiments, Geometric Model, and Calculation Method

2.1. Experiments

The experimental process is shown in Figure 1. All the parameters were based on the experiments performed by the research team before [18]. In this experiment, we used PDC as a substrate. Then we soaked the PDC substrate in the corrosive acid reagents. Table 1 displays the acid agents and the parameters employed in this study.

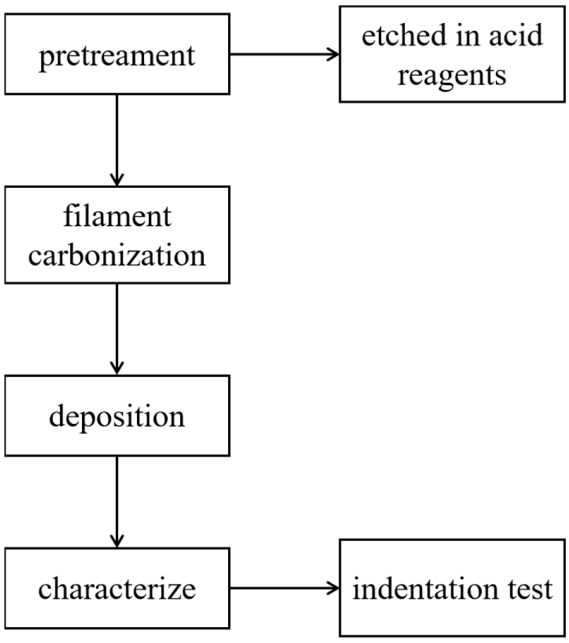

Figure 1. Experimental process.

Table 1. Etching pretreatment parameters of PDC substrate.

Acid Reagents	Concentration Ratio	Temperature/°C	Time/h
H_2SO_4	$V_{H2SO4\ (AR)}$:$V_{H2O2(30\%)}$ = 1:5	25	48

The substrates (both the original and after soaking) were then placed in hot filament CVD (HFCVD) equipment that had been developed by the research team for depositing a diamond coating. We used tungsten filaments(Φ1.0 mm, 4 wires), and chose acetone as the carbon source, and hydrogen as the auxiliary gas. Table 2 displays the parameters of filament carbonization and deposition.

Table 2. Parameters related to filament carbonization and deposition.

Subject	Filament Carbonization	Deposition
gas flow/(mL/min)	1000	1000
carbon concentration/%	4	2
temperature of filament/°C	2100 ± 100	-
distance between filament and substrate/mm	-	9
filament power/kW	3	-
reactive pressure/kPa	6	3
time/h	2	4

The SEM-S-3400 was used to examine the morphology of all the tools utilized. The samples' hardness was assessed using the HBRVU-187.5 Brovey hardness tester (produced by Jinan Fangyuan Testing Instrument Company, Jinan, China), which used a square cone diamond indenter with an opposite surface angle of 136°. The indentation patterns were observed by collecting their SEM images and comparing the bonding strengths between the coating and substrate of the different tools. All the tests were performed under room temperature(about 20 °C) and the humidity was 50% RH [31].

2.2. Geometric Model

In this article, we used PCD as a substrate, and deposited a layer of diamond film on its surface after a certain depth of cobalt removal pretreatment. After the removal of Co, the Co in the surface layer of the substrate was removed, but during the deposition, the Co deep in the substrate would diffuse to the surface of the substrate under high temperature. The remaining holes caused by the removal of Co would not be filled with diamond, and some holes still existed. Therefore, in the modeling process, Co atoms were added to the diamond for doping. Additionally, we deleted the added Co atoms, leaving holes that were similar to the remaining holes after the pretreatment and deposition on the PCD substrate. We used Device Studio software (2023A) to establish the PCD/diamond coating interfacial structures. The addition of Co was achieved by replacing the C atoms in the diamond model, and the holes were added by deleting the atoms in the substrate model.

The modeling process is shown in Figure 2. First, we established a diamond single crystal cell model based on the lattice information in Table 3 (Figure 3), then cut the crystal surfaces (100), (110), (111), and added a vacuum layer (with a thickness of 1.3 nm), and finally, we created a 2 × 2 × 1 supercell model. This model was a CVD diamond coating geometric model. In the same way, we cut out the crystal surfaces (100), (110), (111), added a vacuum layer, and made a supercell, finally randomly replaced 2 C atoms with Co atoms(1#, 2#, 3# samples), this model was a PCD substrate model with different position of Co. When we deleted the Co atoms, we obtained a PCD substrate model with a different position of holes. We combined the CVD diamond coating model with the PCD substrate model with a different position of Co and holes to establish the relevant interface model (Figure 4).

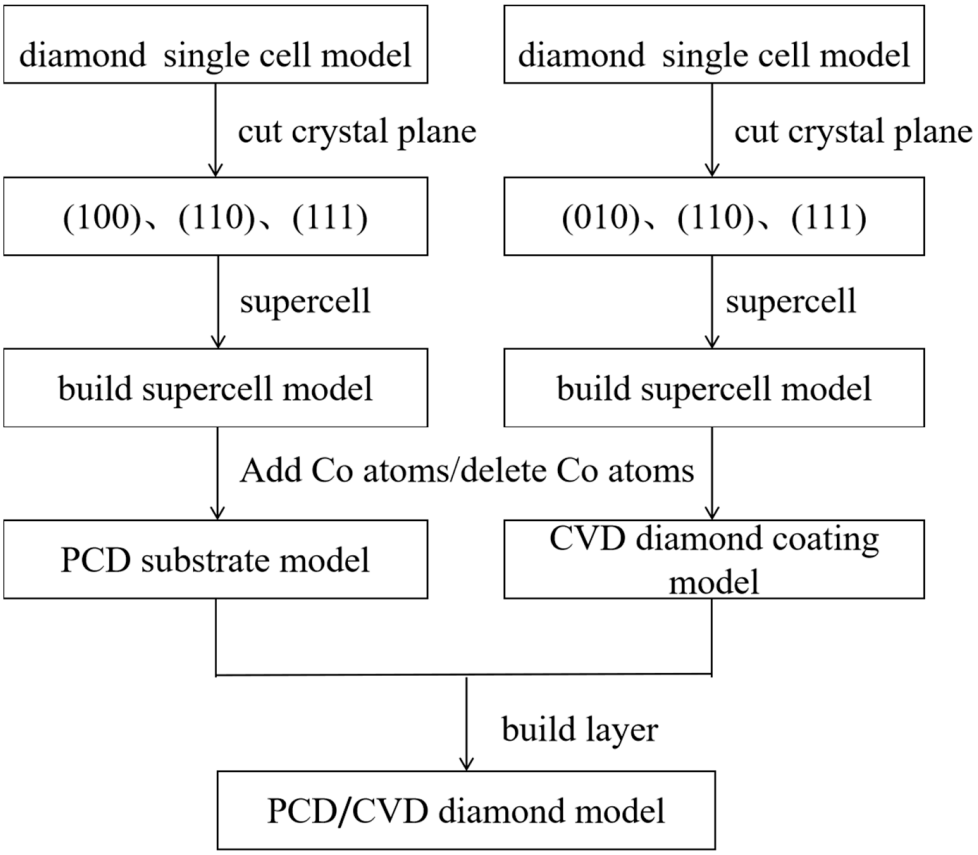

Figure 2. PCD/CVD diamond model building process.

Table 3. Diamond lattice parameters.

Material	Lattice Parameters	Lattice Type
diamond	a = b = c = 3.567 Å, α = β = γ = 90°	face-centered cubic

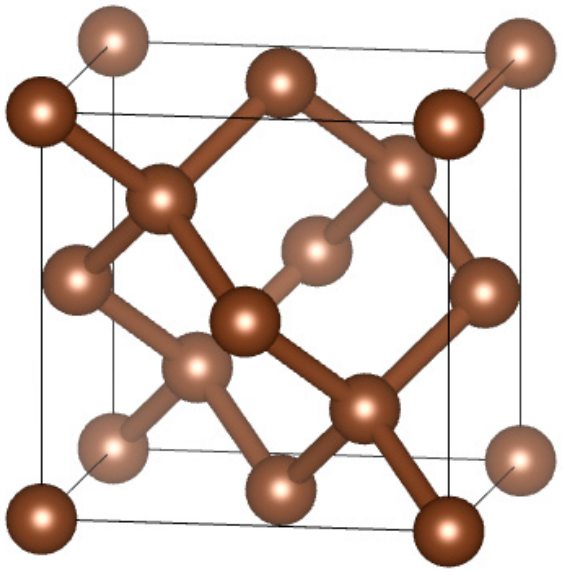

Figure 3. Diamond single crystal cell model.

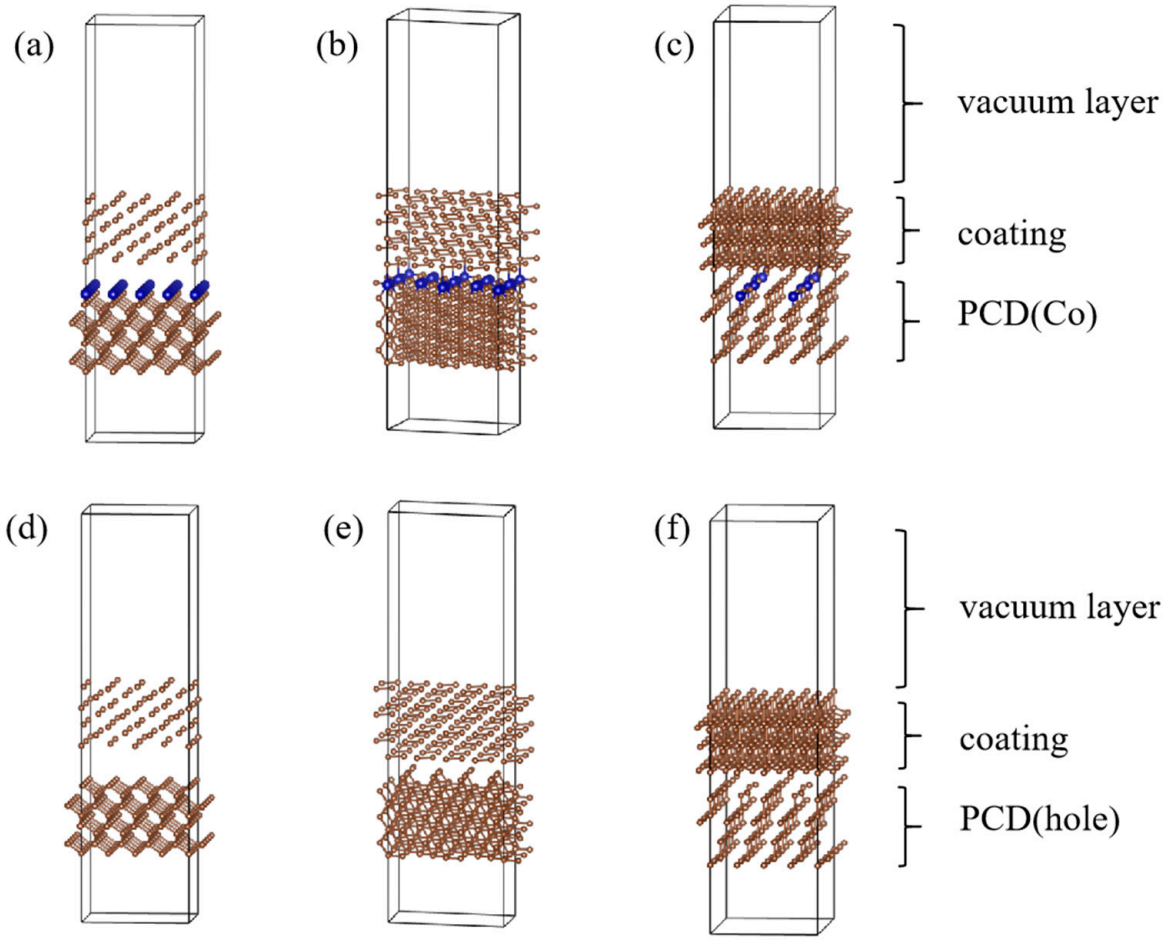

Figure 4. Model of diamond interface with different position of Co and holes: (**a**) Co(100) (1#); (**b**) Co(110) (2#); (**c**) Co(111) (3#); (**d**) hole(100) (4#); (**e**) hole(110) (5#); (**f**) hole(111) (6#).

2.3. Calculation Method

We used DS-PAW software (2023A) package based on the first principles to obtain the most stable structure, then calculated the interficial binding energy, charge density and charge density difference of the diamond-coating interfacial structure with a different position of Co and holes. The exchange potential and the correlation potential were approximated by PBE function modification under the framework of generalized gradient approximation. This used the DFT method combined with the PAW method to explain the interaction between the atomic nucleus and valence electrons. The k-point mesh of the Brillouin zone automatically was set to $4 \times 4 \times 1$ by using the Gamma Center method.

3. Results and Discussion

3.1. Experimental Results and Discussion

Figure 5 shows the indentation images of the CVD diamond coatings when there was Co and holes on the PCD substrate. It could be seen from Figure 5 that both the indentations were relatively obvious, with an obvious pit and clear edges of the indentations. And when the Co was added, the coating indentation was more obvious, indicating that the Co element had a greater impact on the adhesion of the coatings than the holes. This was because the expansion coefficient of cobalt and diamond was large. The higher the cobalt content, the greater the residual stress in the coating, and the easier it was to crack and peel off the coating. However, the effects of the Co elements and holes on the coating adhesion of the different crystal surfaces could not be obtained through experiments.

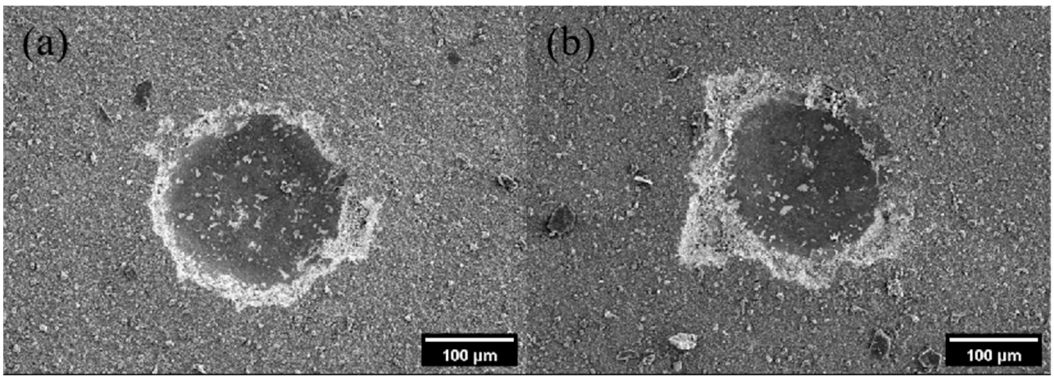

Figure 5. Indentation images of CVD diamond coatings when there were holes (**a**) and Co (**b**) on PCD.

3.2. Calculation and Analysis of Interfacial Binding Energy

Generally, the interfacial binding strength can be quantitatively explained by the interfacial binding energy. The larger the interfacial binding energy, the more stable the interface structure, and the higher the interfacial binding strength. According to article [32], we define the interfacial binding energy between the PCD substrate and diamond coating as follows:

$$W_{ad} = \frac{E_{PCD} + E_{Diamond} - E_{PCD-Diamond}}{A} \quad (1)$$

where W_{ad} is the interfacial binding energy between the PCD substrate and diamond coating, E_{PCD} is the total energy of the PCD substrate, $E_{Diamond}$ is the total energy of the diamond coating, $E_{PCD\text{-}Diamond}$ is the total energy of the diamond coating deposited on the PCD substrate, and A is the cross-sectional area of the interface. Table 4 shows the calculated results of the interfacial binding energy between the PCD substrate and diamond coating with different sites of the Co and holes.

Table 4. PCD/diamond model's energy and interfacial binding energy.

Model	W_{ad}/(eV/nm^2)
1#(100-Co)	26.76
2#(110-Co)	35.17
3#(111-Co)	29.84
4#(100-hole)	0.07
5#(110-hole)	22.62
6#(111-hole)	20.78

The results in Table 4 show that when the Co and holes were located on (110) crystal surface, the interfacial binding energy were 35.17 and 22.62 eV/nm^2, respectively. Obviously, the corresponding adhesive strength of diamond coatings on the (110) surface was the highest, the second was the (111) surface, and the lowest was the (100) surface. This means that the Co and holes had the minimum effect on the interfacial binding energy when on the (110) crystal surface, because the (110) surface was the close-packed faces of diamond crystal. Hence, during the process of preparing PCD, we should make Co exist on the (110) crystal surface of the diamond as much as possible, so that the interfacial binding strength of the tool material can be the highest.

3.3. Analysis of Charge Density of Interface

In order to describe intuitively the interfacial interactions, we calculated the charge density of the most stable structure [33]. Figure 6 shows the interficial charge density between the CVD diamond coating and the PCD substrate with different surfaces. From Figure 6a–c, it could be seen that the charge density was mainly concentrated in the interface for (110) and (111) surface, which means the formation of a typical covalent bond

structure. However, for (100) surface, the charge density obviously tended to concentrate around the Co atom of the PCD substrate and C atom of diamond coatings, indicating that the corresponding interfacial binding strength was week. Because there were certain differences in the ability of Co elements on different crystal surfaces to transfer the charges of its surrounding atoms [34]. Due to the different arrangement of atoms on different crystal surfaces, the number of electrons that Co element can transfer was limited by distance. Further analyzing Figure 6d–f, we could see that when the holes were on the (110) crystal surface, the interfacial charge density was higher than (100) and (111) surfaces. Therefore, the adhesive strength of the diamond coating was the highest. This was consistent with the calculation results of the interficial binding energy.

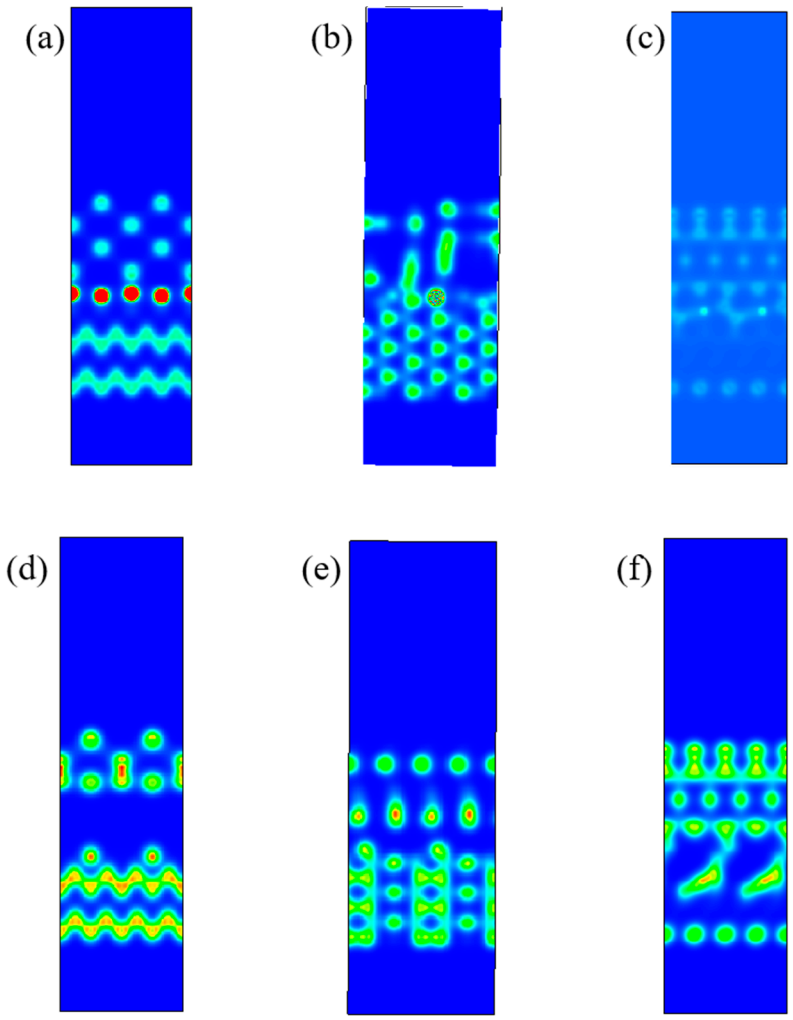

Figure 6. Charge density of diamond interface with different position of Co and holes: (**a**) Co(100) (1#); (**b**) Co(110) (2#); (**c**) Co(111) (3#); (**d**) hole(100) (4#); (**e**) hole(110) (5#); (**f**) hole(111) (6#).

3.4. Analysis of Charge Density Difference of Interface

In order to intuitively characterize the transfer of the charge around the atom, the charge density difference of the interface is usually calculated [35]. Figure 7 shows the charge density difference of the interface between the CVD diamond coating and the PCD substrate with different surfaces. The red and blue regions denote charge accumulation and depletion, respectively. From Figure 7b,e we can clearly see that the upper and lower layers, form a new C-C covalent bond. Furthermore, Co atoms could transfer the charge around C atoms at the interface, when the Co atoms were on the (110) crystal surface, and the phenomenon of charge transfer was the most obvious. At this time, the C-C covalent bond

was the strongest. When the holes were on the (110) crystal surface, the bond strength of the C-C was significantly enhanced. In short, in order to improve the interface binding strength between the PCD substrate and the CVD diamond coating, we must make the Co atoms stay on the (110) crystal surface. The holes were best located on the (110) crystal surface.

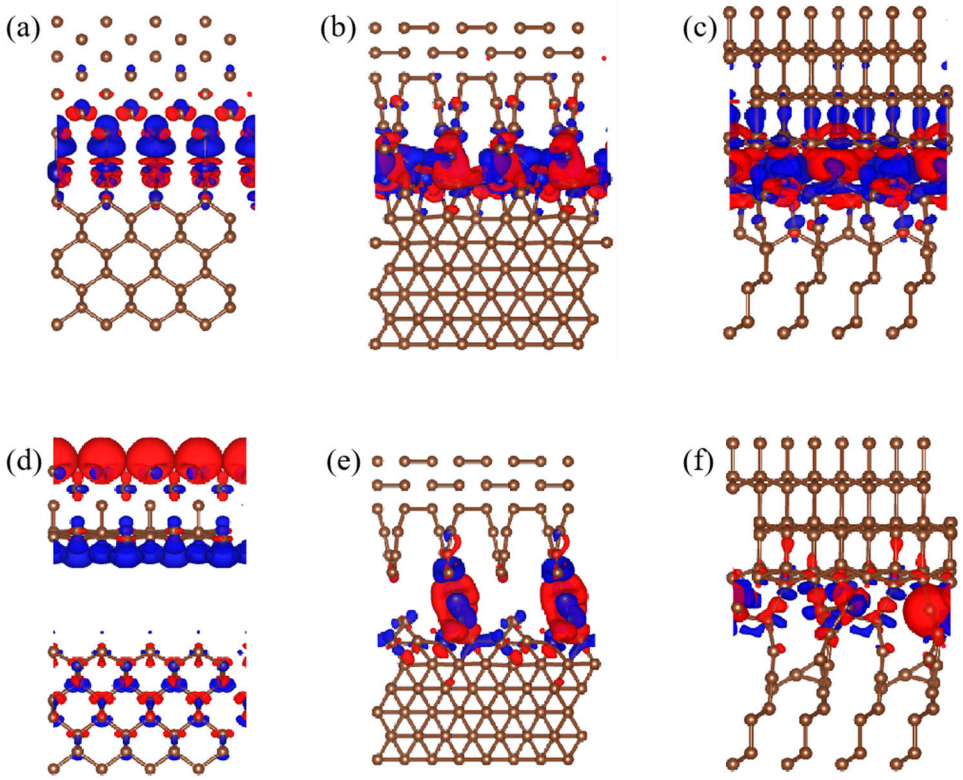

Figure 7. Charge density difference of diamond interface with different position of Co and holes: (**a**) Co(100) (1#); (**b**) Co(110) (2#); (**c**) Co(111) (3#); (**d**) hole(100) (4#); (**e**) hole(110) (5#); (**f**) hole(111) (6#).

4. Conclusions

1. When the Co atoms existed on the (110) crystal surface, the binding energy of the interface between the PCD substrate and the CVD diamond coating was 31.4% higher than the (100) crystal surface and 17.9% higher than the (111) crystal surface. While the holes existed on the (110) crystal surface, the number was 322.1% and 8.9%.
2. Both the Co atoms and holes would affect the charge density and charge transfer of the interface. When the Co atoms and holes were located on the (110) crystal surface, the charge density concentrated mainly in the interface, and the phenomenon of charge transfer was the most obvious. At this time, the C-C covalent bond was the strongest.
3. During the synthesis of PCD, we could regulate the site of the Co binding phase in PCD in the (110) crystal surface, or to remove the Co elements on (110) crystal surfaces during the pretreatment process, or to fill the holes on the (100) and (111) crystal surfaces when depositing, thus the interface binding strength between the PCD substrate and the diamond coatings could be improved.

Author Contributions: Writing—original draft preparation, C.H.; writing—review and editing, G.L. All authors have read and agreed to the published version of the manuscript.

Funding: This research was funded by Hongzhiwei Technology (Shanghai) Co., Ltd. grant number PO2306020790.

Institutional Review Board Statement: Not applicable.

Informed Consent Statement: Not applicable.

Data Availability Statement: The raw/processed data required to reproduce these findings cannot be shared at this time due to legal or ethical reasons.

Acknowledgments: We gratefully acknowledge HZWTECH for providing computation facilities.

Conflicts of Interest: The authors declare that this study received funding from Hongzhiwei Technology (Shanghai) Co., Ltd. The funder was not involved in the study design, collection, analysis, interpretation of data, the writing of this article or the decision to submit it for publication.

References

1. Xiao, C.; Hsia, F.C.; Sutton-Cook, A.; Weber, B.; Franklin, S. Polishing of polycrystalline diamond using synergies between chemical and mechanical inputs: A review of mechanisms and processes. *Carbon* **2022**, *196*, 29–48. [CrossRef]
2. Li, G.; Rahim, M.Z.; Pan, W.; Wen, C.; Ding, S. The manufacturing and the application of polycrystalline diamond tools–A comprehensive review. *J. Manuf. Process.* **2020**, *56*, 400–416. [CrossRef]
3. Xie, D.; Huang, Z.; Yan, Y.; Ma, Y.; Yuan, Y. Application of an innovative ridge-ladder-shaped polycrystalline diamond compact cutter to reduce vibration and improve drilling speed. *Sci. Prog.* **2020**, *103*, 0036850420930971. [CrossRef] [PubMed]
4. Yahiaoui, M.; Gerbaud, L.; Paris, J.Y.; Denape, J.; Dourfaye, A. A study on PDC drill bits quality. *Wear* **2013**, *298–299*, 32–41. [CrossRef]
5. Guignard, J.; Prakasam, M.; Largeteau, A. A review of binderless polycrystalline diamonds: Focus on the high-pressure–high-temperature sintering process. *Materials* **2022**, *15*, 2198. [CrossRef]
6. Gong, W. Study on Carbon Nano-Onion without Additive High Temperature and High Pressure Sintering Polycrystalline Diamond. Master's Thesis, Yanshan University, Qinhuangdao, China, 2012.
7. Guignard, J.; Prakasam, M.; Largeteau, A. High pressure (HP) in spark plasma sintering (SPS) processes: Application to the polycrystalline diamond. *Materials* **2022**, *15*, 4804. [CrossRef]
8. Huang, P.; Wang, W.; Wang, S.; Zhang, X.; Wei, X.; Zhu, Y.; Li, Z. Effect of transition metal carbides on mechanical properties of polycrystalline diamond by HPHT sintering. *Ceram. Int.* **2022**, *48*, 15959–15965. [CrossRef]
9. Qin, W.; Heng, J.; Pei, X.; Li, Z.; Li, X. Study on Co-enhancement of polycrystalline diamond composite sheets. *Diam. Abras. Eng.* **2018**, *38*, 16–20.
10. Fan, P.; Xue, W.; Yi, C.; Dong, P.; Lan, H. Effect of decobalting on thermal stability of polycrystalline diamond. *J. Mater. Sci. Eng.* **2017**, *35*, 87–90+118.
11. Gou, R.; Luo, X.; Xu, G.; Kang, C.; Chen, J.; Zhang, J.; Long, S. Improvement of ambient temperature tribological properties of polycrystalline diamond compact treated by cobalt removal. *Diam. Relat. Mater.* **2021**, *119*, 108567. [CrossRef]
12. Cen, H.; Deng, F.-M.; Guo, Z.-H.; Xiang, B.; Shuang, W.; Xin, Z. Fractal dimension of decobalt surface on PDC with different acid corrosion reagents at room temperature. *Diam. Relat. Mater.* **2020**, *105*, 107699. [CrossRef]
13. Liu, C.; Zhou, F. Effect of soaking time on the friction properties of polycrystalline diamonds. *Int. J. Refract. Met. Hard Mater.* **2015**, *48*, 82–88. [CrossRef]
14. Wang, Q. A Method for Decobalting Complex Acid based on Artificial Polycrystalline Diamond Composite Sheet. CN104532016A, 22 April 2015.
15. Zhou, M.; Duan, Z.; Yan, Y. A Method for Removing Cobalt from Polycrystalline Diamond Composite Sheets. CN105603428A, 25 May 2016.
16. Shao, H. Preparation of D-D Bonded Polycrystalline Diamond and Study on Decobalting Technology. Master's Thesis, Henan Industrial Science, Zhengzhou, China, 2016.
17. Deng, F.-M.; Hao, C.; Deng, W.; Guo, Z.-H.; Bo, X.; Wang, S.; Zhao, X. Effect of different acid corrosion reagents on de-cobalt effect and performance of PDC at room temperature. *Diam. Relat. Mater.* **2020**, *106*, 107702. [CrossRef]
18. Hao, C.; Deng, F.-M.; Guo, Z.; Bo, X.; Wang, S. Study of preparation and cutting performance of a chemical vapor deposition diamond coated cutting tool. *Thin Solid. Film.* **2023**, *771*, 139801.
19. Fan, S.; Kuang, T.; Xu, W.; Zhang, Y.; Su, Y.; Lin, S.; Wang, L. Effect of pretreatment strategy on the microstructure, mechanical properties and cutting performance of diamond coated hardmetal tools using HFCVD method. *Int. J. Refract. Met. Hard Mater.* **2021**, *9*, 105687. [CrossRef]
20. Tao, Z.; Qin, F.A.; Zy, A.; Zhang, L.; Sun, F. Effect of mechanical pretreatment on nucleation and growth of HFCVD diamond films on cemented carbide tools with a complex shape. *Int. J. Refract. Met. Hard Mater.* **2019**, *84*, 105016.
21. Zhang, Z.; Lu, W.; Feng, W.; Du, X.; Zuo, D. Effect of substrate surface texture on adhesion performance of diamond coating. *Int. J. Refract. Met. Hard Mater.* **2020**, *95*, 105402. [CrossRef]
22. Wang, H.; Wang, C.; Wang, X.; Sun, F. Effects of carbon concentration and gas pressure with hydrogen-rich gas chemistry on synthesis and characterizations of HFCVD diamond films on WC-Co substrates. *Surf. Coat. Technol.* **2021**, *409*, 126839. [CrossRef]
23. Lin, Q.; Chen, S.; Ji, Z.; Huang, Z.; Zhang, Z.; Shen, B. A novel growth model for depositing ultrananocrystalline diamond films in CH_4/H_2 chemistry. *Surf. Coat. Technol.* **2021**, *419*, 127280. [CrossRef]
24. Peng, J.; Zeng, J.; Xiao, X.; Li, W. Novel conversion annealing pretreatment for improved deposition of diamond coatings onto WC-Co cemented carbide. *J. Alloys Compd.* **2022**, *893*, 162325. [CrossRef]

25. Jian, X.; He, J.; Wang, J.; Gan, Y. Effect of metal dopant on interface adhesion of diamond coating on impregnated diamond substrate: A first principle calculation. *J. Vac. Sci. Technol.* **2019**, *39*, 58–64.
26. Zhang, K.; Chen, J.; Huang, Z.; Jian, X. Influence of line defect in cemented carbide substrate on bonding strength between diamond coating film and substrate. *Diam. Abras. Eng.* **2017**, *37*, 23–28.
27. Jian, X.; Zhu, Z.; Lei, Q. New progress on the improvement of adhesive strength of HFCVD of diamond coating. *Diam. Abras. Eng.* **2016**, *36*, 11–16.
28. Jian, X.; Chen, J. The Influence of Co binding phase on adhesive strength of diamond coating with cemented carbide substrate. *Acta Phys. Sin.* **2015**, *64*, 368–373.
29. Jian, X.; Zhang, Y. Influence of crystal orientation on adhesive strength of film-substrate interface of diamond coating. *Diam. Abras. Eng.* **2014**, *34*, 1–5.
30. Blöchl, P.E. Projector augmented-wave method. *Phys. Rev. B* **1994**, *50*, 17953–17979. [CrossRef] [PubMed]
31. Adin, M.Ş. A parametric study on the mechanical properties of MIG and TIG welded dissimilar steel joints. *J. Adhes. Sci. Technol.* **2023**, 1–24. [CrossRef]
32. Song, Y.; Xing, F.J.; Dai, J.H.; Yang, R. First-Principles Study of Influence of Ti Vacancy and Nb Dopant on the Bonding of $TiAl/TiO_2$ Interface. *Intermetallics* **2014**, *49*, 1–6. [CrossRef]
33. Li, C.X.; Dang, S.H.; Wang, L.P.; Zhang, C.L.; Han, P.D. Effect of Cr, Mo and Nb Additions on Intergranular Cohesion of Ferritic Stainless steel: First-Principles Determination. *Chin. Phys.* **2014**, *B23*, 37102–37115. [CrossRef]
34. Peng, Y.; Huo, D.; He, H.; Li, Y.; Li, L.; Wang, H.; Qian, Z. Characterization of ZnO: Co Particles Prepared by Hydrothermal Method for Room Temperature Magnetism. *J. Magn. Magn. Mater.* **2012**, *324*, 690–694. [CrossRef]
35. Li, L.; He, S.; Ruan, H.; He, S.; Guo, D. Adhesion and electronic properties of 4H-SiC/α-Al_2O_3 interfaces with different terminations calculated via first-principles methods. *Surf. Interfaces* **2023**, *41*, 103201. [CrossRef]